

Article

Effect of *Cordyceps militaris* Powder Prophylactic Supplementation on Intestinal Mucosal Barrier Impairment and Microbiota-Metabolites Axis in DSS-Injured Mice

Shujian Wu ¹ , Zaoxuan Wu ² and Ye Chen ^{1,2,*}

¹ Shenzhen Clinical Research Center for Digestive Disease, Integrative Microecology Clinical Center, Shenzhen Key Laboratory of Gastrointestinal Microbiota and Disease, Shenzhen Technology Research Center of Gut Microbiota Transplantation, Shenzhen Hospital, Southern Medical University, Shenzhen 518100, China; sjwu@stu2018.jnu.edu.cn

² State Key Laboratory of Organ Failure Research, Department of Gastroenterology, Nanfang Hospital, Southern Medical University, Guangzhou 510080, China; wzx1914458273@163.com

* Correspondence: yechen_fimmu@163.com

Abstract: Ulcerative colitis (UC) is a chronic and recurrent inflammatory disease with an unknown pathogenesis and increasing incidence. The objective of this study is to investigate the impact of prophylactic treatment with *Cordyceps militaris* on UC. The findings demonstrate that prophylactic supplementation of *C. militaris* powder effectively mitigates disease symptoms in DSS-injured mice, while also reducing the secretion of pro-inflammatory cytokines. Furthermore, *C. militaris* powder enhances the integrity of the intestinal mucosal barrier by up-regulating MUC2 protein expression and improving tight junction proteins (ZO-1, occludin, and claudin 1) in DSS-injured mice. Multiomics integration analyses revealed that *C. militaris* powder not only reshaped gut microbiota composition, with an increase in *Lactobacillus*, *Odoribacter*, and *Mucispirillum*, but also exerted regulatory effects on various metabolic pathways including amino acid, glyoxylates, dicarboxylates, glycerophospholipids, and arachidonic acid. Subsequent analysis further elucidated the intricate interplay of gut microbiota, the intestinal mucosal barrier, and metabolites, suggesting that the microbiota–metabolite axis may involve the effect of *C. militaris* on intestinal mucosal barrier repair in UC. Moreover, in vitro experiments demonstrated that peptides and polysaccharides, derived from *C. militaris*, exerted an ability to change the gut microbiota structure of UC patients' feces, particularly by promoting the growth of *Lactobacillus*. These findings suggest that regulatory properties of *C. militaris* on gut microbiota may underlie the potential mechanism responsible for the protective effect of *C. militaris* in UC. Consequently, our study will provide support for the utilization of *C. militaris* as a whole food-based ingredient against the occurrence and development of UC.

Keywords: *Cordyceps militaris*; ulcerative colitis; gut microbiota; metabolites; intestinal mucosal barrier



Citation: Wu, S.; Wu, Z.; Chen, Y. Effect of *Cordyceps militaris* Powder Prophylactic Supplementation on Intestinal Mucosal Barrier Impairment and Microbiota-Metabolites Axis in DSS-Injured Mice. *Nutrients* **2023**, *15*, 4378. <https://doi.org/10.3390/nu15204378>

Academic Editors: Ruggiero Francavilla and Jean-Louis Guéant

Received: 5 September 2023

Revised: 4 October 2023

Accepted: 13 October 2023

Published: 16 October 2023



Copyright: © 2023 by the authors. Licensee MDPI, Basel, Switzerland. This article is an open access article distributed under the terms and conditions of the Creative Commons Attribution (CC BY) license (<https://creativecommons.org/licenses/by/4.0/>).

1. Introduction

With rapid diets and lifestyle changes, Inflammatory Bowel Disease (IBD) has progressively become a growing challenge to public health in the world. Ulcerative colitis (UC), a subtype of IBD, is characterized by clinical symptoms such as abdominal pain and bloody diarrhea, significantly influencing the quality of life. At the turn of the 21st century, the prevalence rates of UC were recorded at 505 per 100,000 in Norway (Europe), 286 per 100,000 in the USA (North America), 57 per 100,000 in Japan (Eastern Asia), and 196 per 100,000 in Barwon (Oceania) [1]. The global incidence and prevalence of UC are rising, while its pathogenesis remains unclear [1,2]. Despite the availability of several biological agents for the treatment of UC, response and remission rates remain unsatisfactory in approximately 60% of cases [3]. Therefore, it is necessary to explore more effective ways and approaches to alleviate UC.

Increasing evidence has revealed a strong association between gut microbiota and the intestinal mucosal barrier in relation to UC [4–6]. The intestinal mucosal barrier plays a critical role in preventing the entry of and responding to harmful contents [7]. Numerous studies have reported that intestinal mucosal barrier dysfunction is an early event in UC [8]. Moreover, existing data clearly imply that gut microbiota dysbiosis plays a central role in the pathogenesis of UC [6,9,10]. The integrity and function of the intestinal mucosal barrier may be damaged by gut microbiota dysbiosis, thereby promoting the proliferation of the pathogenic bacteria and secretion of enterotoxins, resulting in an increase in the intestinal permeability and intestinal immune dysregulation, eventually leading to the onset of chronic intestinal inflammation [6]. Therefore, it is a potential therapeutic target for UC to balance gut microbiota and regulate the intestinal mucosal barrier function.

Most mushrooms, rich in biocomponents, are not easily digestible and/or absorbed in the upper gastrointestinal tract, but are excellent sources of prebiotics to interact with gut microbiota [11]. *Cordyceps militaris* (CM), a medicinal mushroom, is cultured *Cordyceps sinensis* mycelium, which is widely used in many Asian countries [12]. Previous studies have demonstrated that CM powder exhibited an ability to regulate the immune system in humans [13] and protect mice from triptolide-induced acute hepatotoxicity [12]. Recent studies also highlighted the potential of active constituents from CM to ameliorate type 2 diabetes mellitus, obesity, and neurodegenerative diseases, through modulating gut microbiota and improving intestinal mucosal structure damage [14–16]. However, multiple biocomponents of CM may have potential synergistic effects, and it remains unclear whether CM can alleviate UC by regulating the intestinal mucosal barrier and gut microbiota. Therefore, this study aims to investigate the prophylactic supplementation effect of CM on DSS-induced UC in mice and its impact on gut microbiota structure, through in vitro fermentation of UC patients' feces. We attempt to explore the effects of CM on the explicit mechanisms of gut microbiota, the intestinal mucosal barrier, and UC.

2. Materials and Methods

2.1. Animals and Treatments

Thirty-two male C57BL/6 mice, aged 6–7 weeks and weighing 20 ± 2 g, were obtained from Sibeifubio Biotechnology Co., Ltd. (Beijing, China), and housed in an environment with a temperature of 24 ± 2 °C and a light/dark cycle of 12 h, with food and water provided ad libitum. After 1 week for adaptation, the mice were randomly divided into four groups ($n = 8$). CM and dextran sodium sulfate (DSS) were obtained from Guangdong Fudonghai Pharmaceutical Co., Ltd. (Zhanjiang, China) and MP Biomedicals Co., Ltd. (Irvine, CA, USA), respectively. As illustrated in Figure 1A, the control group was treated with sterile water, whereas the high-dose CM group (HCM + DSS) and low-dose CM group (LCM + DSS) received CM powder at 300 mg/kg BW/day and 100 mg/kg BW/day (using 0.1% hydroxymethyl cellulose as a vehicle) by oral gavage once daily for 14 days, respectively. Meanwhile, the model group (Veh + DSS) received the same amount of 0.1% hydroxymethyl cellulose once daily. From days 7 to 14, mice in all groups except the control group were administered 2.5% (w/v) DSS in drinking water to induce colitis. At the end of the experiment, mice were anesthetized with ether, and blood samples were collected by enucleation of the eyeballs. The samples were then centrifuged at 4 °C and $3000 \times g$ for 20 min to obtain the serum. Subsequently, the mice were then euthanized by cervical dislocation. The colon length was measured, and distal colon tissues (approximately 1.5 cm) were fixed with 4% paraformaldehyde before the tissue sections were prepared.

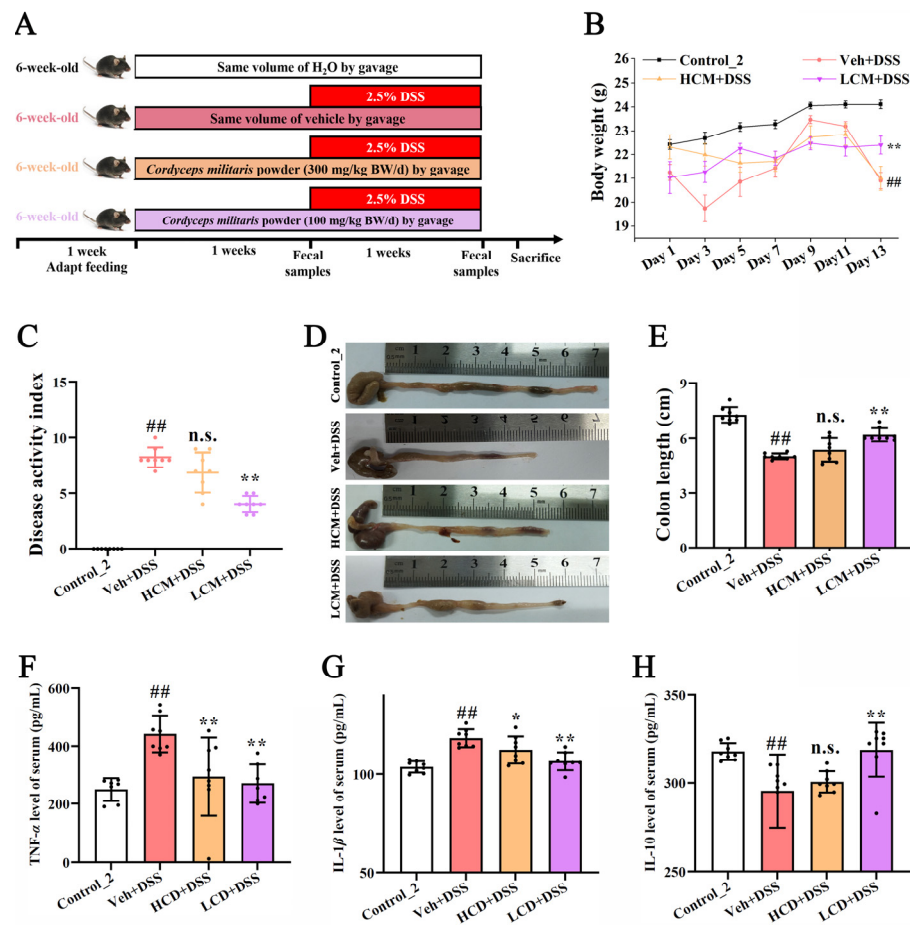


Figure 1. Effects of CM powder on the symptoms of mice with DSS-induced ulcerative colitis ($n = 8$). (A) Schematic representation of experimental protocol. (B) Body weight. (C) DAI score. (D,E) Colon length. (F–H) The levels of TNF- α , IL-1 β , and IL-10 in the serum. ##, $p < 0.01$ versus control group; *, $p < 0.05$ versus model group; **, $p < 0.01$ versus model group; n.s., no significant difference ($p > 0.05$).

2.2. Histopathological Examination and Evaluation of Colons

The distal colon was dehydrated and embedded in paraffin, then cut into 5- μ m slices and stained with a hematoxylin and eosin (H&E) stain. Histopathological changes were examined using a microscope (NIKON, Tokyo, Japan).

2.3. Disease Activity Index and Histological Score

The disease activity index (DAI) score and histological score (HS) of the colons were calculated according to Tables 1 and 2.

Table 1. Disease activity index (DAI) scoring criteria.

| Body Weight Loss | Stool Consistency for Diarrhea | Fecal Occult Blood | Score |
|------------------|--------------------------------|---------------------------------------|-------|
| None | Normal | Normal | 0 |
| 1–5% | Soft but still formed | Melena and negative blood | 1 |
| 6–10% | Soft | Positive blood | 2 |
| 11–15% | Soft and wet | Blood stains can be seen on the stool | 3 |
| >15% | Watery diarrhea | Rectal bleeding | 4 |

The DAI is expressed as the average of these scores.

Table 2. Histological score (HS) criteria.

| Inflammation | Mucosal Damage | Crypt Loss | Pathological Change Range | Score |
|--------------|---------------------|--------------------------------|---------------------------|-------|
| None | None | None | None | 0 |
| Mild | Mucus layer | 1–33% | 1–25% | 1 |
| Moderate | Submucosa | 34–66% | 26–50% | 2 |
| Severe | Muscular and serosa | 67–100% + intact epithelium | 51–75% | 3 |
| - | - | 100% with epithelium lose | 76–100% | 4 |

The HS is expressed as the average of these scores.

2.4. Cytokine Analysis of Serum

The levels of IL-1 β , TNF- α , IL-6, and proteins were analyzed using the commercially available kits, according to the manufacturers' instructions (Mlbio, Shanghai, China).

2.5. Immunofluorescence Assessment

The paraffin sections of the colon tissues were obtained in the same way as the H&E stain. After dewaxing and hydration, 3 μ m thick slices were subjected to antigen repair and 5% BSA closure. The sections were then incubated overnight at 4 $^{\circ}$ C with an anti-rabbit MUC2 antibody (Abclonal, Woburn, MA, USA, A14659), anti-rabbit occludin (CST, 91131S), anti-rabbit claudin 1 antibody (Proteintech, Rosemont, IL, USA, 13050-1-AP), and an anti-rabbit ZO-1 antibody (Proteintech, 21773-1-AP), respectively. Subsequently, they were incubated for 1 h at 37 $^{\circ}$ C with Alexa Fluor 488-labelled goat antirabbit secondary antibody (Beyotime, A0423), and covered with an anti-fluorescence quenching sealing solution containing DAPI (Beyotime, Shanghai, China) for 1 h at room temperature. Finally, the images were captured using a fluorescence microscope and analyzed using ImageJ software (1.6).

2.6. 16S rRNA Gene Sequencing for Fecal Matter

Fecal samples were collected from each mouse at 7 days (time 1, T1), which were labelled as control_1 group, Veh group, HCM group, and LCM group. Fecal samples were also collected from each mouse at 14 days (time 2, T2), which were labelled as control_2 group, Veh + DSS group, HCM + DSS group, and LCM + DSS group.

The genomic DNA of the mouse fecal samples at T1 and T2 was obtained using the E.Z.N.A. soil DNA kit (Omega Bio-Tek, Norcross, GA, USA). The extracted DNA was amplified by PCR in the V3-V4 hypervariable region. The primers were 341F (5'-CCTAYGGGRBGCASCAG-3') and 806R (5'-CCTAYGGGRBGCASCAG-3'). Sequencing was performed using the Illumina MiSeq PE300 platform/NovaSeq PE250 platform (Illumina, San Diego, CA, USA), according to the standard procedure of Majorbio Bio-Pharm Technology Co., Ltd. (Shanghai, China).

2.7. Untargeted Fecal Metabolomics Analysis

Untargeted metabolomic profiling of feces at T2 was conducted by Biotree Biotech Co., Ltd. (Shanghai, China). A 25 mg sample was mixed with a 500 μ L extraction solvent (acetonitrile/methanol, 1:1) containing an isotopically labelled internal standard. Next, the mixture was vortexed for 30 s and subjected to ultrasound treatment for 10 min. After resting at -40 $^{\circ}$ C for 1 h, the supernatant was obtained by centrifugation at 13,800 \times g for 15 min at 4 $^{\circ}$ C. The supernatant was then analyzed by LC-MS/MS with a UHPLC system (Vanquish, Thermo Fisher Scientific, Waltham, MA, USA), coupled to an Orbitrap Exploris 120 mass spectrometer (Orbitrap MS, Thermo Fisher Scientific, Waltham, MA, USA), utilizing a Waters ACQUITY UPLC BEH Amide column (2.1 mm \times 100 mm, 1.7 μ m). The mobile phases of A and B were water and acetonitrile, respectively. The temperature and injection volume were set at 4 $^{\circ}$ C and 2 μ L, respectively. The quality control (QC) sample was prepared by mixing an equal aliquot of the supernatant of samples. The Betaine-

(trimethyl-d9) hydrochloride, L-leucine-5,5,5-d3, Trimethylamine-d9 N-Oxide, Hippuric acid-d5, [13C3]-L-(+)-sodium lactate, and L-leucine-5,5,5-d3 was the internal standard.

The raw data were obtained under both positive and negative ion models, and then converted to the mzXML format using ProteoWizard, processed with an in-house program developed using R and based on XCMS for peak detection, extraction, alignment, and integration. The metabolites were authenticated by searching an in-house MS2 database (Biotree DB (v2.1)). The metabolites were annotated when the MS2 score was >0.3.

2.8. *In Vitro* Fermentation of Peptides and Polysaccharides from CM

The peptides and polysaccharides were obtained from CM [14,15,17,18]. The CM powder was extracted with water. Next, the supernatant was precipitated using ethanol and ammonium sulfate. Then, it was dialyzed and lyophilized to obtain the proteins and polysaccharides. The proteins and polysaccharides were further digested *in vitro* using simulated gastrointestinal digestion with pepsin and pancreatin.

Four volunteers of patients with active UC (2 females and 2 males, aged 30–40 years, China) provided fecal samples. The fresh feces (5.0 g with anaerobic bags) were mixed with PBS (pH = 7, 0.15% cysteine) at a ratio of 1:4 (g/mL), and then centrifuged at $500\times g$ for 5 min at 4 °C. Afterwards, the supernatant, as a bacterial suspension for fermentation, was collected and stored at –80 °C before use.

The fermentation process and the preparation of the *in vitro* fermentation medium were performed according to a previous method. Briefly, 1 mL bacterial suspension was mixed with 4 mL culture medium in each anaerobic tube. The peptides and polysaccharides were added into the anaerobic tubes at a concentration of 5 mg/mL, respectively. The fermentation process was performed under anaerobic conditions with 37 °C and 60 rpm. Samples were collected at 0, 6, 12, and 24 h by centrifugation ($12,000\times g$, 12 min). The precipitation was analyzed for 16S rRNA gene sequencing.

2.9. Statistical Analysis

Data were presented as means \pm SD or SEM. Statistical analysis was conducted with IBM SPSS 19.0 software, using a one-way analysis of variance (ANOVA) test with Duncan's multiple range test ($p < 0.05$). Graph design was performed using GraphPad Prism 8.0.2 software and Origin 9. The intensity of the fluorescence was analyzed by using the Image J software.

3. Results

3.1. CM Powder Alleviated DSS-Induced UC in Mice

After two weeks (Figure 1), compared to the control_2 group, the body weights of the DSS-injured mice were reduced by 13.28%, while the low dose CM powder treatment (7.02%) significantly inhibited weight loss ($p < 0.01$) (Figure 1B). As the DAI score (Figure 1C) and colon length (Figure 1D,E) showed, a significant increase in DAI score and an obvious reduction in colon length were observed in the Veh + DSS group ($p < 0.01$). Notably, the adverse symptoms in the LCM + DSS group were significantly improved ($p < 0.01$). Moreover, pro-inflammatory cytokines (TNF- α and IL-1 β) and anti-inflammatory cytokines (IL-10) played an important role in UC [19]. A reduction in TNF- α and IL-1 β and an increase in IL-10 were observed in the LCM + DSS group (Figure 1F–H). Collectively, these findings implied that CM powder could alleviate the disease symptoms in DSS-injured mice.

3.2. CM Powder Enhanced Intestinal Mucosal Barrier Function

The intact intestinal mucosal barrier plays an important role in preventing bacterial invasion and physical damage, which is critical in UC [20]. As shown in Figure 2A, there were no histopathological changes in the control_2 group with an intact mucosa and abundant goblet cells. In contrast, severe damage to the epithelial surface, mucosal inflammation, extensive inflammatory cell infiltration, goblet cell exhaustion, and crypt distortion were observed in the DSS-treated mice. However, treatment with the low dose

of CM powder attenuated these pathological changes, indicating that the colonic structure damages were repaired in DSS-induced UC mice.

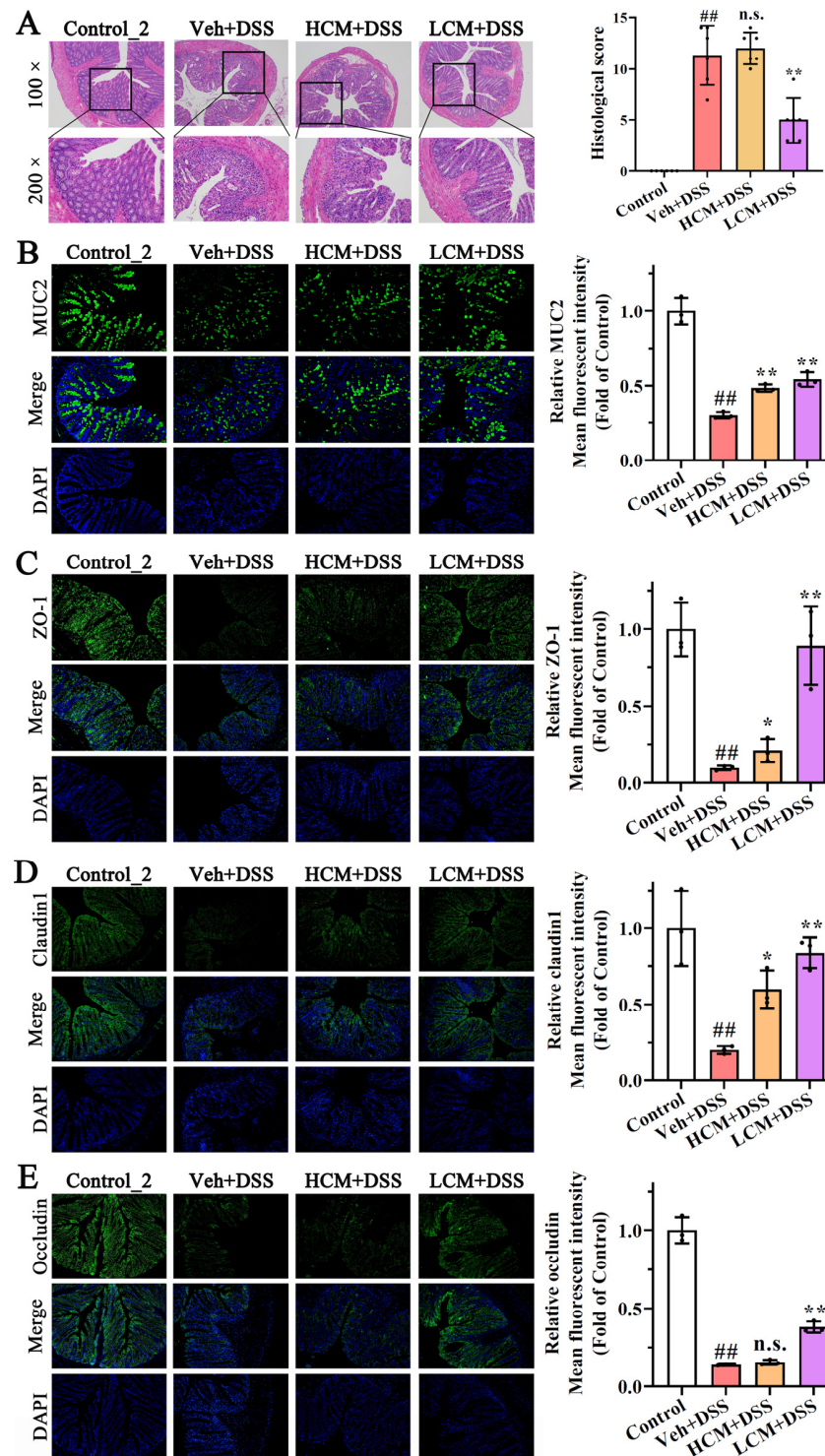


Figure 2. Effects of CM powder on intestinal mucosal barrier in DSS-induced ulcerative colitis mice. (A) Representative images of H&E staining (magnification of 100× and 200×) and its histopathological evaluation ($n = 8$). (B–E) Representative images (magnification of 200×) of immunofluorescence staining of MUC2, ZO-1, claudin 1, and occludin, and its mean fluorescent intensity ($n = 3$). All images were taken at the same scale. ##, $p < 0.01$ versus control group; *, $p < 0.05$ versus model group; **, $p < 0.01$ versus model group; n.s., no significant difference ($p > 0.05$).

The immunofluorescence analysis showed that the levels of MUC2, ZO-1, claudin 1, and occludin were markedly down-regulated in DSS-induced UC mice ($p < 0.01$), whereas CM powder treatment increased the levels of MUC2, ZO-1, claudin 1, and occludin in the distal colon both of the HCM + DSS group and the LCM + DSS group (Figure 2). Notably, there were no statistically significant differences in the HS and the level of occludin protein between the Veh + DSS group and the HCM + DSS group. Compared to the HCM + DSS group, a higher level of MUC2, ZO-1, and claudin 1 was observed in the LCM + DSS group. These results suggest that the CM powder treatment had an excellent protective effect on the intestinal mucosal barrier function of DSS-injured mice, especially the low dose CM powder treatment.

3.3. CM Powder Intervention Changed the Fecal Microbiota Composition

A total of 3,622,264 and 3,538,725 raw reads were obtained from 24 samples at T1 and T2, respectively. After identification and removal of the chimeric sequences, 1581 and 1834 OTUs with a 97% similarity level were obtained, respectively. The rank abundance (Figure S1A), Shannon index, and rarefaction curves (Figure S1B), and the coverage index (Figure S1C,D) indicated that the sequencing depth covers most of the bacterial diversity, including rare new phylotypes. Compared to the control_1 group, the richness (Chao index, Figure 3A) and diversity (Shannon index, Figure 3A) were enhanced by hydroxymethyl cellulose and CM powder treatment at T1. However, the different groups were not separate, but rather intermingled with the overall region in principal coordinate analysis (PCoA) (Figure 3A), indicating that there was no statistical difference between the groups. The results suggested that CM powder could affect the gut microbiota structure but tended to be similar to control_1 group at T1. After the mice were exposed to DSS, compared to the control_2 group, the richness was decreased in the Veh + DSS group; the control_2 group and the Veh + DSS group separated from each other in PCoA, outside the overall region at T2 (Figure 3B), indicating a significant change in the gut microbiota composition in DSS-induced UC. On the other hand, CM powder can enhance the richness and diversity in DSS-injured mice (Figure 3B), and obvious differences were observed among the Veh + DSS group, HCM + DSS group, and LCM + DSS group (PCoA, Figure 3B). Hence, a prophylactic treatment of CM powder can influence the gut microbiota composition in DSS-induced UC.

The OTUs of the HCM + DSS group and the LCM + DSS group were enhanced at T2, compared to DSS-injured mice. There were 261, 107, 162, and 176 unique OTUs in the control_2 group, Veh + DSS group, HCM + DSS group, and LCM + DSS group, respectively (Figure S1E). Additionally, the Firmicutes/Bacteroidetes (F/B) ratio is an important indicator of gut microbiota dysbiosis [15]. The F/B ratio decreased in the Veh + DSS group compared to the control_2 group, while the CM powder treatment prevented a decrease in the F/B ratio in the HCM + DSS group and LCM + DSS group (Figure 3C). These findings imply that the CM powder treatment effectively improved gut microbiota dysbiosis in UC. At the phylum level and genus level, Firmicutes, Bacteroidota, Desulfobacterota, and Proteobacteria were the most common bacterial phylum in all groups. Among them, Firmicutes and Bacteroidota accounted for more than 90% of the total microbiota in each group at phylum level (Figure 3D). *Norank_f_Muribaculaceae*, *norank_f_norank_o_Clostridia_UCG-014*, *Bacteroides*, *Phascolarctobacterium*, *Lachnospiraceae_NK4A136_group*, and *unclassified_f_Lachnospiraceae* were the topmost abundant microbiota in all experimental groups at the genus level (Figure S1F). The linear discriminant analysis effect size (LEfSe) was performed to uncover the differences between the Veh + DSS group and LCM + DSS group (from the phylum to genus level). The linear discriminant analysis (LDA, score > 2.0) showed that the change in gut microbiota in relative abundance was caused by 16 dominant communities in the Veh + DSS group and 26 dominant communities in the LCM + DSS group (Figure 3E). At genus level, *norank_f_Muribaculaceae*, *Akkermansia*, *Defluviitaleaceae_UCG-011*, and *Marvinbryantia* were abundant in the Veh + DSS group. The low dose CM powder intervention significantly altered the abundances of *uncultured_f_Ruminococcaceae*, *Mucispirillum*, *Lactobacillus*, *Desulfovibrio*, *unclassified_f_Prevotellaceae*, *Parvibacter*, *Odoribacter*, *Harryflintia*, UCG-007,

unclassified_f__Sutterellaceae, *Monoglobus*, and *Faecalibaculum* in DSS-injured mice. Therefore, the alteration of gut microbiota using a low dose of CM powder may be critical for the alleviation of UC.

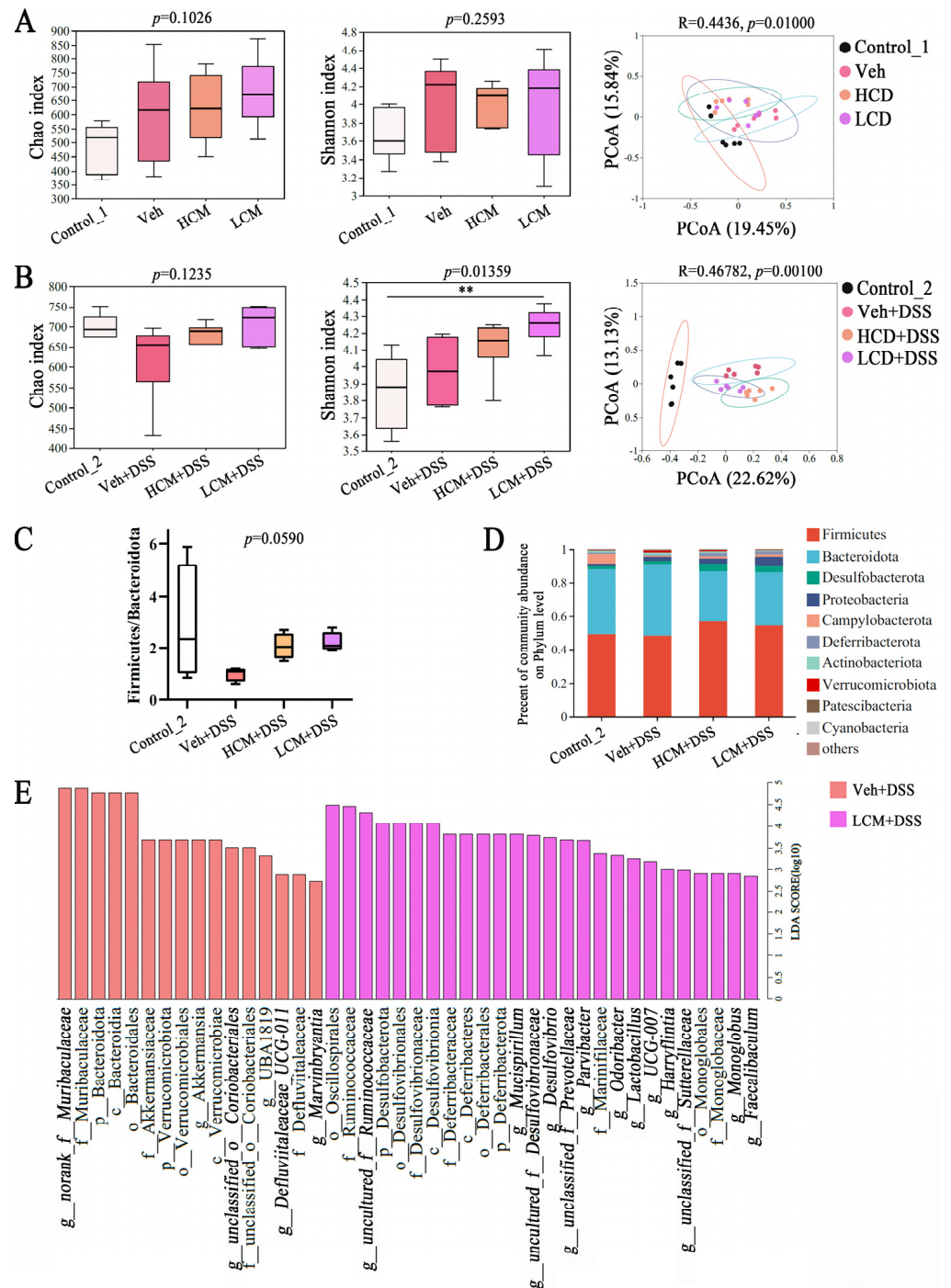


Figure 3. Effects of CM powder on gut microbiota at T1 and T2 ($n = 6$). **(A)** Chao index, Shannon index, and the principal coordinate analysis (PCoA) at the OTU level of different groups at T1. **(B)** Chao index, Shannon index, and PCoA at the OTU level of different groups at T2. **(C)** The ratio of Firmicutes/Bacteroidetes of different groups at genus level of group at T2. **(D)** The community bar plots at the phylum level at T2. **(E)** The LefSe analyses from genus to phylum at the genus level at T2. **, means significant difference between two group ($p < 0.01$).

3.4. CM Powder Modulated the Fecal Metabolome in DSS-Injured Mice

The fecal metabolome was further analyzed using untargeted metabolomics. The OPLS-DA model showed that there was a good predictability and did not overfit, according to $p < 0.05$ and R^2Y values of 0.99 and 0.97 in control_2 vs. Veh + DSS and Veh + DSS vs. LCM + DSS, respectively (Figure S2A). The principal component analysis (PCA) showed an obvious separation trend in control_2 vs. Veh + DSS and Veh + DSS vs. LCM + DSS, implying that significant differences existed in fecal metabolites among the different experimental groups (Figure S2B). Significant differential metabolites were identified based on a threshold of $VIP > 1$ and $p < 0.05$ from all groups, including lipids and lipid-like molecules (31.37%), organic acids and derivatives (25.64%), organoheterocyclic compounds (13.87%), organic oxygen compounds (7.99%), and others (21.12%) (Figure S2C). The K-means clustering analysis shows that nine distinct clusters of differential metabolites were determined based on the variation tendency, which indicated great differences in metabolites following treatment using DSS and CM powder. DSS induced a decreasing tendency in clusters 2, clusters 3, and clusters 8, and an increasing tendency in clusters 6 and clusters 7 compared to control_2, while a low dose CM powder treatment reversed the tendency (Figure 4A), revealing that CM powder treatment affected the gut microbiota-derived metabolites significantly.

There were 167 and 50 significantly differential metabolites (with accurate names in the database) in control_2 vs. Veh + DSS and Veh + DSS vs. LCM + DSS (Table S1). Compared to the control_2 group, 69 metabolites were up-regulated, while 98 were down-regulated in the Veh + DSS group (Table S1 and Figure S2D). Compared to the Veh + DSS group, 37 metabolites were up-regulated while 13 were down-regulated in the LCM + DSS group (Table S1 and Figure S2C). Among them, 20 commonable differential metabolites (CDMs) existed between the control_2 vs. Veh + DSS and Veh + DSS vs. LCM + DSS (Figure 4B). Thirty exclusive differential metabolites (EDMs) were only observed in the Veh + DSS vs. LCM + DSS. Phenylethylamine, PC(22:5(7Z,10Z,13Z,16Z,19Z)/18:1(11Z)), 2,4-Pentadienal, pyrrolidine, succinic acid, indoleacetic acid, dodecanedioic acid, 5'-Deoxy-5'-methylthioadenosine, (Alpha-D-mannosyl)7-beta-D-mannosyl-diacetylchitobiosyl-L-asparagine, isoform A (protein), and hydroxypyruvic acid were the top 10 significant differential metabolites in Veh + DSS vs. LCM + DSS (Figure 4C and Table S2). Notably, the low dose CM powder treatment reversed the up-regulation of eight metabolites and the down-regulation of twelve metabolites of CDMs in DSS-injured mice, when compared to the control_2 group. Twenty-five metabolites were increased and five metabolites were reduced in EDMs, which were not observed in the control_2 vs. Veh + DSS. Additionally, the metabolic pathway analysis of KEGG-enriched pathways showed that significantly differential metabolites of Veh + DSS vs. LCM + DSS involved the pathways of ATP binding cassette (ABC) transporters (19.05%), glycerophospholipid metabolism (14.29%), neuroactive ligand–receptor interaction (9.52%), amino acid metabolism (9.52%), arachidonic acid metabolism (9.52%), galactose metabolism (9.52%), and choline metabolism in cancer (9.52%) (Figure 4D). Based on enrichment analysis and topological analysis, the biosynthesis and degradation of valine, leucine, and isoleucine and the metabolism of tryptophan, phenylalanine, tyrosine, glycine, serine, threonine, starch, sucrose, sphingolipid, glyoxylate, dicarboxylate, and arachidonic were the key pathways with the highest correlation for significantly differential metabolites of Veh + DSS vs. LCM + DSS, particularly amino acid metabolism (Figure 4E). Thus, the CM powder treatment affected metabolic pathways significantly.

Gut microbiota had a significant interactions with disease signs (including body weight, colon length, and the histological score of colons) (Figure 5A) and indicators of the intestinal mucosal barrier (Figure 5B). *Lactobacillus*, *Limosilactobacillus*, and *Ligilactobacillus* were negatively correlated with the HS of colon. *Lactobacillus*, *Limosilactobacillus*, *uncultured_f_Lachnospiraceae*, and *Ligilactobacillus* were positively correlated with body weight and colon length. Moreover, *Turicibacter*, *Dubosiella*, and *norank_f_Eubacterium_coprostanoligenes_group* were positively correlated with TNF- α and IL-1 β (Figure 5C). *Lactobacillus*, *Rikenella*, *Limosilactobacillus*, and *Ligilactobacillus* were negatively correlated with TNF- α and IL-1 β (Figure 5C). As shown in Figure 5D, Firmicutes is the main phylum that was significantly associated with the modulation of metabolites, including *Ligilactobacillus*, *Turicibacter*, *Anaerostipes*, *Lactobacillus*, *norank_f_Eubacterium_coprostanoligenes_group*, *uncultured_f_Ruminococcaceae*, *Dubosiella*, *uncultured_f_Lachnospiraceae*, *Limosilactobacillus*, *norank_f_norank_o_Clostridia_UCG-014*, and *Phascolarctobacterium*. Moreover, *Bacteroides*, *Alistipes*, *Prevotellaceae_UCG-001*, *Escherichia-Shigella*, *uncultured_f_Desulfovibrionaceae*, and *Mucispirillum* also had a clearly positive and/or negative correlation with special differential metabolites. Interestingly, the low dose CM powder treatment improved the changes in glycerophospholipids in CDMs (Figure S3A). According to the VIF < 10 of glycerophospholipids (Table S3), Spearman’s correlation analysis of gut microbiota and three glycerophospholipids showed that *uncultured_f_Lachnospiraceae*, *Lactobacillus*, *Limosilactobacillus*, and *Lachnospiraceae_NK4A136_group* were positively correlated with the three glycerophospholipids, respectively (Figure S3B). *Dubosiella*, *Turicibacter*, *Alistipes*, *norank_f_Eubacterium_coprostanoligenes_group*, *Phascolarctobacterium*, *norank_f_norank_o_Clostridia_UCG-014*, and *norank_f_Muribaculaceae* were negatively correlated with the three glycerophospholipids, respectively (Figure S3B). These results implied that the effect of CM powder on UC was related to the interaction among gut microbiota, metabolites, and intestinal mucosal barrier.

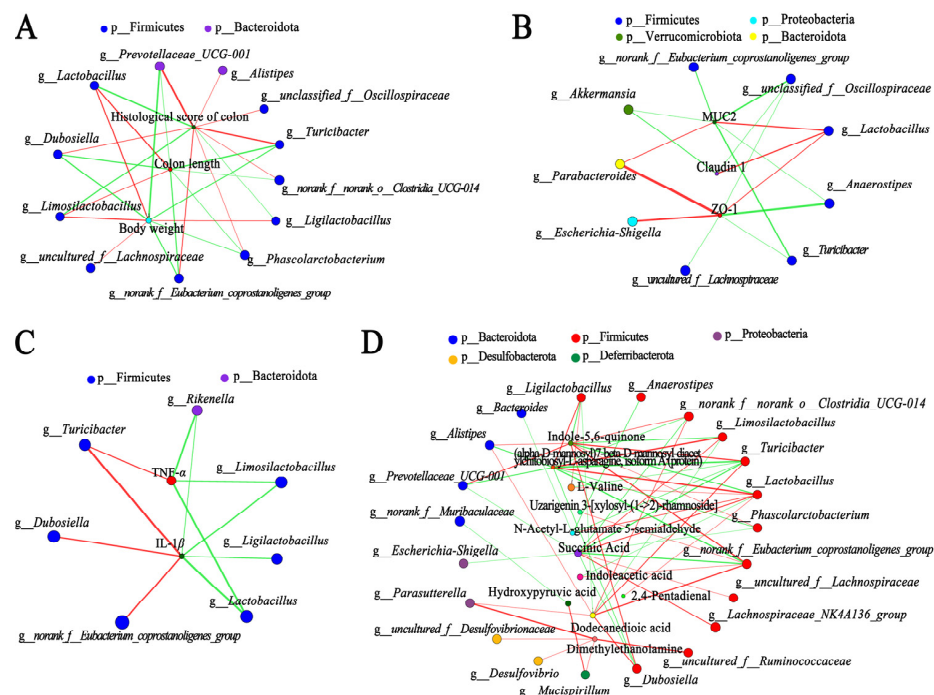


Figure 5. Correlation among gut microbiota, metabolites, and other parameters. (A) Network diagram showing relationships between gut microbiota and disease signs. (B) Network diagram showing relationships between gut microbiota and indicators of intestinal mucosal barrier. (C) Network of correlation analysis between gut microbiota and cytokines. (D) Network of correlation analysis between gut microbiota and special metabolites. In Network diagrams, the node size represents species abundance, the line thickness represents the correlation coefficient, the red line represents a positive correlation, and the green line represents a negative correlation. The correlation analysis of Heatmap and Network was carried out by Spearman’s correlation coefficients.

3.6. Peptides and Polysaccharides of CM Changed the Gut Microbiota Structure of UC Patient's Faeces

The major active compounds with a high content of CM are polysaccharides (~40%) and proteins/peptides (~30%) [12,14,15,21]. To further investigate the regulatory effect of CM on the gut microbiota in humans, the structure of UC patients' feces gut microbiota was analyzed by fermenting peptides and polysaccharides from CM. As showed in Figure 6A, the 0 h group was significantly different from each sample treatment group, and there was no obvious overall region among all experimental groups in PCoA, implying that peptides and polysaccharides of CM significantly altered the structure of the gut microbiota during fermentation. Furthermore, peptides and polysaccharides with CM intervention enhanced the abundances of *Lactobacillus* after 24 h of fermentation, particularly peptides ($p < 0.01$) (Figure 6B,C). A significant reduction in *Rothia* and *Actinomyces* was observed during fermentation with treatment using peptides and polysaccharides.

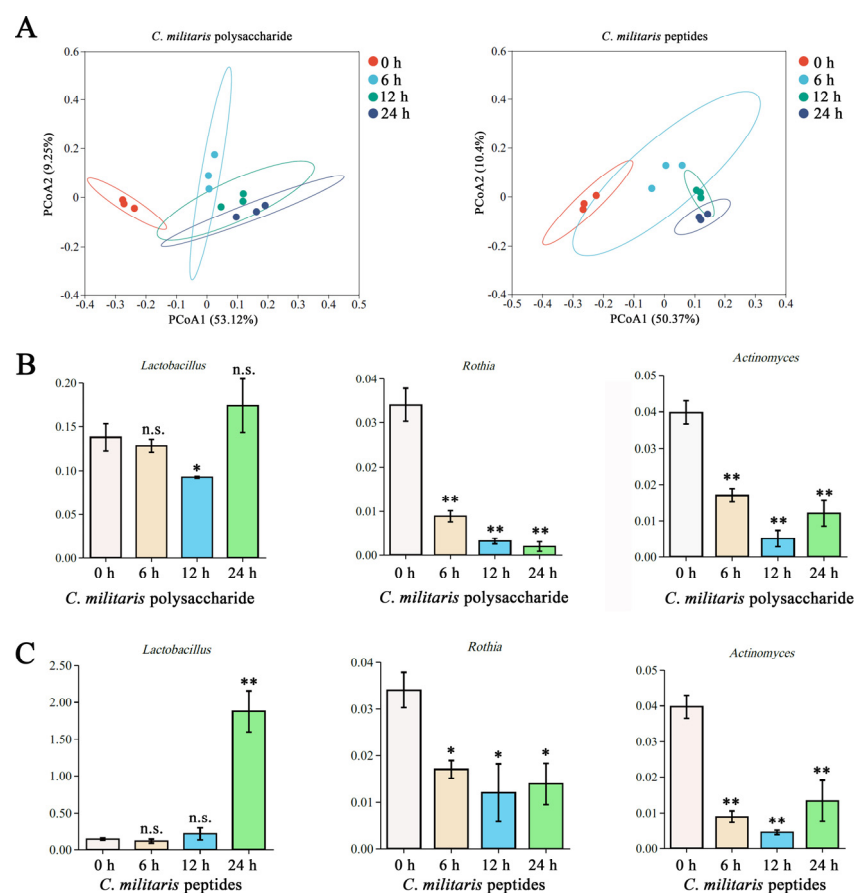


Figure 6. Response of the gut microbiota in UC patient's faeces to fermentation of CM polysaccharides and peptides. (A) PCoA of microbial composition. (B,C) Variation in specific genera by polysaccharide and peptides, including *Lactobacillus*, *Rothia*, and *Actinomyces*. *, $p < 0.05$ versus 0 h group; **, $p < 0.01$ versus 0 h group; n.s., no significant difference ($p > 0.05$).

4. Discussion

The anti-inflammatory effects of edible plants have been reported in various studies [22], while only a few studies focused on the effects of edible mushrooms on UC. This study explored the effect of prophylactic supplementation of CM powder on UC in mice. Generally, weight loss, diarrhea, bloody stool, and inflammation levels were indirect markers of UC [23,24]. Inflammation, congestion, and edema of the colon could cause a decrease in colon length which is related to the severity of UC [15,24,25]. Surprisingly, prophylactic supplementation with CM powder significantly improved UC-related symptoms, inhibited the increase in TNF- α and IL-1 β in serum, and prevented a decrease in IL-10. Importantly,

the animal dose (100 mg/kg BW/day) of CM can be extrapolated to a human equivalent theoretical dose of consuming about 0.5 g per day (based on a body weight of 60 kg) [26], which is reasonably achievable in a human diet. Therefore, the inclusion of whole CM powder in the diet at an appropriate dose is a potential prebiotic to intervene in UC, encouraging us to further investigate the mechanisms by which whole CM powder relieves UC. Undoubtedly, recommended intake levels and toxicologic investigations of CM need to be researched in further studies.

Abnormalities in intestinal mucosal barriers are likely an early event in the pathogenesis of UC [8,27]. Dysfunction of intestinal mucosal barriers may increase the permeability, subsequently exacerbating the invasion of intestinal commensal microbes and toxins, resulting in a persistent inappropriate immune response that promotes chronic inflammation [28]. In the present study, CM powder improved the adverse symptoms caused by damage to the structure of the intestinal mucosal barrier. Moreover, MUC2 is produced by intestinal goblet cells in the epithelial cell layer and dominated the mucus layer as part of intestinal mucosal barrier [29]. Mucosal inflammation was negatively correlated with the concentration of MUC2 in UC patients [30]. Simultaneously, research has also shown that the intestinal mucosal barrier is mainly regulated by epithelial TJ proteins [20]. Claudin and occludin form homotypic complexes between epithelial cells, and ZO-1 connects occludin and claudin to the actin cytoskeleton, in order to maintain the integrity of the structure and the normal functioning of the intestinal mucosal barrier [31]. Taken together, the loss of MUC2 and TJ proteins may be key to the destruction of the intestinal mucosal barrier destruction in this study. Thus, prophylactic supplementation with CM powder effectively mitigates the impairment of the intestinal mucosal barrier in DSS-induced UC, by up-regulating MUC2 and TJ proteins.

Some studies have reported that gut microbiota dysbiosis is associated with the pathogenesis and development of UC [6,32]. The gut microbiota mediated the intestinal immunity response, inflammatory response, and intestinal mucosal barrier function to intervene in UC [33]. Diet is one of the inevitable factors affecting gut microbiota, which is closely related to UC. There were no statistically significant differences between the model group and the sample treatment groups in gut microbiota composition at T1 (Figure 3A), while the CM powder treatment enhanced the abundance of beneficial bacteria (*Lactobacillus*, *Odoribacter*, and *Mucispirillum*) in DSS-injured mice at T2, implying that prophylactic treatment with CM powder subsequently affects the gut microbiota structure during DSS exposure. More importantly, *Lactobacillus* is one of the probiotics that maintains intestinal health, as it can regulate intestinal homeostasis, host immunity, and activation of the aryl hydrocarbon receptor (AhR) pathway against intestinal mucosal barrier damage in UC [34,35]. *Mucispirillum* and *Odoribacter* are protective species to improve UC symptoms [36,37]. *Mucispirillum* can trigger T-cell-dependent immunoglobulin A and immunoglobulin G, and their subsequent immune responses [36,38]. *Odoribacter* have an ability to protect cells from UC [37,39]. Moreover, short-chain fatty acids (SCFAs) are a well-known bacterial metabolite with anti-inflammatory effects. *Lactobacillus* and *Odoribacter* can produce SCFAs to exert their probiotic effects on the intestinal mucosal barrier [15,37,40]. Furthermore, the integrity of the intestinal mucosal barrier depends on its interactions with gut microbiota. The impairment of the intestinal mucosal barrier is closely associated with the uncontrollable immune reaction and/or the unrestricted dysbiosis of gut microbiota in the intestine [41]. The gut microbiota at the outer mucus layer not only modulates mucus layer dynamics, but also mediates mucin production and secretion to maintain mucus barrier integrity [42]. *Lactobacillus* can strengthen the functions of the intestinal mucosal barrier, through enhancing goblet cells and Paneth cells, promoting the formation and expression of TJs, and increasing immune barrier functions [43]. *Mucispirillum* is involved as a mucus associated niche in the distal colon, which may be important to forming a functional protective intestinal mucus layer [44]. Zhao et al. found that an increase in *Odoribacter* is positively correlated with the intestinal mucosal barrier and inflammatory responses, contributing to attenuating DSS-induced colitis [45]. Summarily, the regulating properties

of gut microbiota and their potential effects on intestinal mucosal barrier function are the key to CM powder resisting UC.

Gut microbiota-derived metabolites have important effects on metabolic and nutritional homeostasis and immune system maturation and stimulation [34]. Microbial metabolites are the connecting links between gut microbiota and the host's health in UC, as they modulate immune and metabolic responses to interferences with gut homeostasis and disease progression [32]. The correlation analysis displays significant interactions between gut microbiota and metabolites in this study. Amino acid metabolism is an important enrichment pathway of significantly differential metabolites. Previous research has proved that the feces of patients with UC had different degrees of changes in various amino acids, such as a reduction in valine and glutamate expression and an enhancement of tryptophan and isoleucine content [46,47]. Generally, the difference in microbial metabolites in DSS-injured mice are mainly concentrated in amino acid metabolism, which may contribute to the differential expressions of mucin and mucus [47]. Zhu et al. demonstrated that a Tanshinone IIA treatment mainly improved DSS-induced UC by altering the metabolisms of amino acid, arachidonic acid, glyoxylate, and dicarboxylate [48]. Our metabolomics analysis also is consistent with these results. Thus, the microbiota–metabolites axis is one of the critical pathways for CM powder against UC.

It should be noted that the abundance of *Lactobacillus* was obviously enhanced by CM powder. *Lactobacillus* was not only negatively correlated with TNF- α , IL-1 β , and the HS of the colon, but was also positively correlated with MUC2, claudin 1, and ZO-1. Furthermore, the enrichment metabolic pathway involved tryptophan metabolism in this study. Accumulating data suggest that *Lactobacillus* metabolizes dietary tryptophan to activate the aromatic hydrocarbon receptor pathway; this may be an important way to regulate intestinal homeostasis and host immunity, including gut barrier protection and immune modulation [34]. Interestingly, oral administration of CM powder could directly improve the DSS-induced change in glycerophospholipids, which has a clear correlation with gut microbiota. Yuan et al. reported that Huang-Lian Jie-Du decoction mainly modulates the arachidonic acid metabolic pathway and the glycerophospholipid metabolic pathway to alleviate UC, which are involved in inhibiting cyclooxygenase-2 protein expression and the activity of phospholipase A2 and 5-lipoxygenase [49]. These findings suggested that the effects of CM powder on the microbiota–metabolites axis in UC are worth further study in the future, particularly focusing on the pathway of *Lactobacillus* and the metabolic pathways of amino acid and glycerophospholipid in repairing the intestinal mucosal barrier.

In fact, the biological activity of edible plants is closely related to their active compounds. The total content of protein and polysaccharides were >70% in CM [12,21]. In the present study, an in vitro fermentation model revealed that the gut microbiota structure was changed significantly by the peptides and polysaccharides of CM, which may be a major factor for the effect of the regulatory properties of CM on the gut microbiota. Notably, *Rothia* and *Actinomyces* could be considered biomarkers in patients with active UC [50]. A lower level of *Lactobacillus* and higher levels of *Rothia* and *Actinomyces* in patients with active UC, compared to in healthy controls, were reported in a clinical study [50]. In contrast, our results found that peptides and polysaccharides from CM enhanced *Lactobacillus* (beneficial bacteria) and reduced *Rothia* and *Actinomyces* (harmful bacteria) in UC patients' feces. These results suggest that peptides and polysaccharides from CM had the ability to regulate gut microbiota in the fecal samples of UC patients. The effects of the regulatory properties of CM on gut microbiota in UC may be the result of the potential synergistic effects of peptides and polysaccharides. Our data provide further evidence for the effects of the regulatory properties of CM on gut microbiota and the efficacy of CM as a dietary supplement for UC prevention in humans.

5. Conclusions

The present research demonstrated that prophylactic treatment of CM could effectively mitigate gut microbiota dysbiosis and intestinal mucosal barrier damage in DSS-induced UC mice. Further analysis showed that CM regulates gut microbiota and subsequently affects metabolic pathways, which may be involved in the intestinal mucosal barrier repair in order to alleviate UC, involving the abundance of *Lactobacillus*, *Odoribacter*, and *Mucispirillum*, and the metabolic pathways of amino acid metabolism, glyoxylate and dicarboxylate metabolism, and arachidonic acid metabolism. Furthermore, peptides and polysaccharides from CM can alter gut microbiota structure in feces samples from UC patients. In summary, our results reveal that CM could act as a potential and economical prebiotics to improve UC, via modulating the microbiota–metabolites axis and repairing the intestinal mucosal barrier, which also provides a holistic perspective for dietary intake and gut microbiota homeostasis in the disease progression of UC.

Supplementary Materials: The following supporting information can be downloaded at: <https://www.mdpi.com/article/10.3390/nu15204378/s1>; Figure S1: differences in the composition of gut microbial and diversity analysis at T1 and T2; Figure S2: metabonomic analysis of faeces; Figure S3: correlation analysis of glycerophospholipids; Table S1: the statistical information of differential metabolisms among different groups under positive and negative electrospray ionization modes (VIP > 1 and $p < 0.05$); Table S2: detailed information for significantly different metabolites; Table S3: variance inflation factor (VIF) of different environmental factors for correlation analysis.

Author Contributions: Conceptualization, S.W. and Z.W.; methodology, S.W.; software, Z.W.; validation, S.W. and Z.W.; formal analysis, S.W.; investigation, S.W.; resources, Y.C.; data curation, S.W.; writing—original draft preparation, S.W.; writing—review and editing, Y.C.; visualization, S.W. and Z.W.; supervision, Y.C.; project administration, Y.C.; funding acquisition, Y.C. All authors have read and agreed to the published version of the manuscript.

Funding: This work was supported by the National Natural Science Foundation of China (82070543 and 82270581), the National Key R&D Program of China (2021YFA0717001), Shenzhen Science and Technology Planning Project (KCFZ20211020163558024), and Shenzhen Science and Technology Program (ZDSYS20220606100800002).

Institutional Review Board Statement: All experimental animals and experiments were approved by the Ethics Committee of Shenzhen Hospital of Southern Medical University on Laboratory Animal Care (No.2023-0051). All volunteers with UC were well-informed, and the protocols of this study were approved by the Ethics Committee of Nanfang Hospital of Southern Medical University (NFEC-2014-035).

Informed Consent Statement: Informed consent was obtained from all subjects involved in the study.

Data Availability Statement: The data presented in this study are available on request from the corresponding author. The data are not publicly available due to respect of patient privacy.

Conflicts of Interest: The authors declare no conflict of interest.

References

1. Ng, S.C.; Shi, H.Y.; Hamidi, N.; Underwood, F.E.; Tang, W.; Benchimol, E.I.; Panaccione, R.; Ghosh, S.; Wu, J.; Chan, F.; et al. Worldwide incidence and prevalence of inflammatory bowel disease in the 21st century: A systematic review of population-based studies. *Lancet* **2017**, *390*, 2769–2778. [[CrossRef](#)]
2. Shivaji, U.N.; Nardone, O.M.; Cannatelli, R.; Smith, S.C.; Ghosh, S.; Iacucci, M. Small molecule oral targeted therapies in ulcerative colitis. *Lancet Gastroenterol. Hepatol.* **2020**, *5*, 850–861. [[CrossRef](#)]
3. Ferretti, F.; Cannatelli, R.; Monico, M.C.; Maconi, G.; Ardizzone, S. An Update on Current Pharmacotherapeutic Options for the Treatment of Ulcerative Colitis. *J. Clin. Med.* **2022**, *11*, 2302. [[CrossRef](#)] [[PubMed](#)]
4. Yu, J.; Zhao, J.; Xie, H.; Cai, M.; Yao, L.; Li, J.; Han, L.; Chen, W.; Yu, N.; Peng, D. Dendrobium huoshanense polysaccharides ameliorate ulcerative colitis by improving intestinal mucosal barrier and regulating gut microbiota. *J. Funct. Food* **2022**, *96*, 105231. [[CrossRef](#)]
5. Zhou, F.; Lin, Y.; Chen, S.; Bao, X.; Fu, S.; Lv, Y.; Zhou, M.; Chen, Y.; Zhu, B.; Qian, C.; et al. Ameliorating role of Tetrastigma hemsleyanum polysaccharides in antibiotic-induced intestinal mucosal barrier dysfunction in mice based on microbiome and metabolome analyses. *Int. J. Biol. Macromol.* **2023**, *241*, 124419. [[CrossRef](#)]

6. Zou, J.; Liu, C.; Jiang, S.; Qian, D.; Duan, J. Cross Talk between Gut Microbiota and Intestinal Mucosal Immunity in the Development of Ulcerative Colitis. *Infect. Immun.* **2021**, *89*, e1421. [[CrossRef](#)]
7. Huang, L.; He, F.; Wu, B. Mechanism of effects of nickel or nickel compounds on intestinal mucosal barrier. *Chemosphere* **2022**, *305*, 135429.
8. van der Post, S.; Jabbar, K.S.; Birchenough, G.; Arike, L.; Akhtar, N.; Sjøvall, H.; Johansson, M.E.V.; Hansson, G.C. Structural weakening of the colonic mucus barrier is an early event in ulcerative colitis pathogenesis. *Gut* **2019**, *68*, 2142–2151. [[CrossRef](#)]
9. Hill, J.H.; Round, J.L. SnapShot: Microbiota effects on host physiology. *Cell* **2021**, *184*, 2796. [[CrossRef](#)] [[PubMed](#)]
10. Wu, S.; Bhat, Z.F.; Gounder, R.S.; Ahmed, I.A.M.; Al-Juhaimi, F.Y.; Ding, Y.; Bekhit, A.E.D.A. Effect of Dietary Protein and Processing on Gut Microbiota—A Systematic Review. *Nutrients* **2022**, *14*, 453. [[CrossRef](#)]
11. Yadav, D.; Negi, P.S. *Chapter 30—Role of Mushroom Polysaccharides in Improving Gut Health and Associated Diseases*; Bagchi, D., Downs, B.W., Eds.; Microbiome, Immunity, Digestive Health and Nutrition Academic Press: Houston, TX, USA, 2022; pp. 431–448.
12. Wang, L.; Huang, Q.; Huang, Y.; Xie, J.; Qu, C.; Chen, J.; Zheng, L.; Yi, T.; Zeng, H.; Li, H. Comparison of protective effect of ordinary *Cordyceps militaris* and selenium-enriched *Cordyceps militaris* on triptolide-induced acute hepatotoxicity and the potential mechanisms. *J. Funct. Food* **2018**, *46*, 365–377. [[CrossRef](#)]
13. Sun, Y.; Shao, Y.; Zhang, Z.; Wang, L.; Mariga, A.M.; Pang, G.; Geng, C.; Ho, C.; Hu, Q.; Zhao, L. Regulation of human cytokines by *Cordyceps militaris*. *J. Food Drug Anal.* **2014**, *22*, 463–467. [[CrossRef](#)]
14. Huang, R.; Zhu, Z.; Wu, S.; Wang, J.; Chen, M.; Liu, W.; Huang, A.; Zhang, J.; Wu, Q.; Ding, Y. Polysaccharides from *Cordyceps militaris* prevent obesity in association with modulating gut microbiota and metabolites in high-fat diet-fed mice. *Food Res. Int.* **2022**, *157*, 111197. [[CrossRef](#)]
15. Wu, S.; Wu, Q.; Wang, J.; Li, Y.; Chen, B.; Zhu, Z.; Huang, R.; Chen, M.; Huang, A.; Xie, Y.; et al. Novel Selenium Peptides Obtained from Selenium-Enriched *Cordyceps militaris* Alleviate Neuroinflammation and Gut Microbiota Dysbiosis in LPS-Injured Mice. *J. Agric. Food Chem.* **2022**, *70*, 3194–3206. [[CrossRef](#)]
16. Liu, X.; Dun, M.; Jian, T.; Sun, Y.; Wang, M.; Zhang, G.; Ling, J. *Cordyceps militaris* extracts and cordycepin ameliorate type 2 diabetes mellitus by modulating the gut microbiota and metabolites. *Front. Pharmacol.* **2023**, *14*, 1134429. [[CrossRef](#)] [[PubMed](#)]
17. Zhu, Z.; Huang, R.; Huang, A.; Wang, J.; Liu, W.; Wu, S.; Chen, M.; Chen, M.; Xie, Y.; Jiao, C.; et al. Polysaccharide from *Agrocybe cylindracea* prevents diet-induced obesity through inhibiting inflammation mediated by gut microbiota and associated metabolites. *Int. J. Biol. Macromol.* **2022**, *209*, 1430–1438. [[CrossRef](#)] [[PubMed](#)]
18. Wu, S.; Chen, M.; Liao, X.; Huang, R.; Wang, J.; Xie, Y.; Hu, H.; Zhang, J.; Wu, Q.; Ding, Y. Protein hydrolysates from *Pleurotus geesteranus* obtained by simulated gastrointestinal digestion exhibit neuroprotective effects in H₂O₂-injured PC12 cells. *J. Food Biochem.* **2022**, *46*, e13879. [[CrossRef](#)] [[PubMed](#)]
19. Soufli, I.; Toumi, R.; Rafa, H.; Touil-Boukoffa, C. Overview of cytokines and nitric oxide involvement in immuno-pathogenesis of inflammatory bowel diseases. *World J. Gastrointest. Pharmacol. Ther.* **2016**, *7*, 353–360. [[CrossRef](#)] [[PubMed](#)]
20. Wang, K.; Wu, L.; Dou, C.; Guan, X.; Wu, H.; Liu, H.; Oz, H. Research Advance in Intestinal Mucosal Barrier and Pathogenesis of Crohn's Disease. *Gastroenterol. Res. Pract.* **2016**, *2016*, 9686236–9686238. [[CrossRef](#)]
21. Yu, X.; Zou, Y.; Zheng, Q.; Lu, F.; Li, D.; Guo, L.; Lin, J. Physicochemical, functional and structural properties of the major protein fractions extracted from *Cordyceps militaris* fruit body. *Food Res. Int.* **2021**, *142*, 110211. [[CrossRef](#)]
22. Lu, Q.; Li, R.; Yang, Y.; Zhang, Y.; Zhao, Q.; Li, J. Ingredients with anti-inflammatory effect from medicine food homology plants. *Food Chem.* **2022**, *368*, 130610. [[CrossRef](#)]
23. Hu, Q.; Yuan, B.; Wu, X.; Du, H.; Gu, M.; Han, Y.; Yang, W.; Song, M.; Xiao, H. Dietary Intake of *Pleurotus eryngii* Ameliorated Dextran-Sodium-Sulfate-Induced Colitis in Mice. *Mol. Nutr. Food Res.* **2019**, *63*, e1801265. [[CrossRef](#)]
24. Li, M.; Ge, Q.; Du, H.; Jiang, P.; Bao, Z.; Chen, D.; Lin, S. Potential Mechanisms Mediating the Protective Effects of *Tricholoma matsutake*-Derived Peptides in Mitigating DSS-Induced Colitis. *J. Agric. Food Chem.* **2021**, *69*, 5536–5546. [[CrossRef](#)]
25. Liu, F.; Wang, X.; Li, D.; Cui, Y.; Li, X. Apple polyphenols extract alleviated dextran sulfate sodium-induced ulcerative colitis in C57BL/6 male mice by restoring bile acid metabolism disorder and gut microbiota dysbiosis. *Phytother. Res.* **2021**, *35*, 1468–1485. [[CrossRef](#)]
26. Reagan-Shaw, S.; Nihal, M.; Ahmad, N. Dose translation from animal to human studies revisited. *FASEB J.* **2008**, *22*, 659–661. [[CrossRef](#)] [[PubMed](#)]
27. Dorofeyev, A.E.; Vasilenko, I.V.; Rassokhina, O.A.; Kondratiuk, R.B.; Amre, D. Mucosal Barrier in Ulcerative Colitis and Crohn's Disease. *Gastroenterol. Res. Pract.* **2013**, *2013*, 431231–431239. [[CrossRef](#)] [[PubMed](#)]
28. Wu, H.; Chen, Q.Y.; Wang, W.Z.; Chu, S.; Liu, X.X.; Liu, Y.J.; Tan, C.; Zhu, F.; Deng, S.J.; Dong, Y.L.; et al. Compound sophorae decoction enhances intestinal barrier function of dextran sodium sulfate induced colitis via regulating notch signaling pathway in mice. *Biomed. Pharmacother.* **2021**, *133*, 110937. [[CrossRef](#)] [[PubMed](#)]
29. Yao, D.; Dai, W.; Dong, M.; Dai, C.; Wu, S. MUC2 and related bacterial factors: Therapeutic targets for ulcerative colitis. *EBioMedicine* **2021**, *74*, 103751. [[CrossRef](#)]
30. Van Klinken, B.J.; Van der Wal, J.W.; Einerhand, A.W.; Buller, H.A.; Dekker, J. Sulphation and secretion of the predominant secretory human colonic mucin MUC2 in ulcerative colitis. *Gut* **1999**, *44*, 387–393. [[CrossRef](#)]
31. Seo, K.; Seo, J.; Yeun, J.; Choi, H.; Kim, Y.; Chang, S. The role of mucosal barriers in human gut health. *Arch. Pharm. Res.* **2021**, *44*, 325–341.

32. Zeng, W.; He, D.; Xing, Y.; Liu, J.; Su, N.; Zhang, C.; Wang, Y.; Xing, X. Internal connections between dietary intake and gut microbiota homeostasis in disease progression of ulcerative colitis: A review. *Food Sci. Hum. Wellness* **2021**, *10*, 119–130. [[CrossRef](#)]
33. Guo, X.Y.; Liu, X.J.; Hao, J.Y. Gut microbiota in ulcerative colitis: Insights on pathogenesis and treatment. *J. Dig. Dis.* **2020**, *21*, 147–159. [[CrossRef](#)] [[PubMed](#)]
34. Huang, Z.; Xie, L.; Huang, L. Regulation of host immune responses by *Lactobacillus* through aryl hydrocarbon receptors. *Med. Microecol.* **2023**, *16*, 100081. [[CrossRef](#)]
35. Dhillon, P.; Singh, K. Therapeutic applications of probiotics in ulcerative colitis: An updated review. *Pharmanutrition* **2020**, *13*, 100194. [[CrossRef](#)]
36. Nan, Q.; Ye, Y.; Tao, Y.; Jiang, X.; Miao, Y.; Jia, J.; Miao, J. Alterations in metabolome and microbiome signatures provide clues to the role of antimicrobial peptide KT2 in ulcerative colitis. *Front. Microbiol.* **2023**, *14*, 1027658. [[CrossRef](#)]
37. Wan, J.; Yu, X.; Liu, J.; Li, J.; Ai, T.; Yin, C.; Liu, H.; Qin, R. A special polysaccharide hydrogel coated on *Brasenia schreberi*: Preventive effects against ulcerative colitis via modulation of gut microbiota. *Food Funct.* **2023**, *14*, 3564–3575. [[CrossRef](#)]
38. Bunker, J.J.; Flynn, T.M.; Koval, J.C.; Shaw, D.G.; Meisel, M.; McDonald, B.D.; Ishizuka, I.E.; Dent, A.L.; Wilson, P.C.; Jabri, B.; et al. Innate and Adaptive Humoral Responses Coat Distinct Commensal Bacteria with Immunoglobulin A. *Immunity* **2015**, *43*, 541–553. [[CrossRef](#)]
39. Lima, S.F.; Gogokhia, L.; Viladomiu, M.; Chou, L.; Putzel, G.; Jin, W.; Pires, S.; Guo, C.; Gerardin, Y.; Crawford, C.V.; et al. Transferable Immunoglobulin A-Coated *Odoribacter splanchnicus* in Responders to Fecal Microbiota Transplantation for Ulcerative Colitis Limits Colonic Inflammation. *Gastroenterology* **2022**, *162*, 166–178. [[CrossRef](#)]
40. Peng, L.; Gao, X.; Nie, L.; Xie, J.; Dai, T.; Shi, C.; Tao, L.; Wang, Y.; Tian, Y.; Sheng, J. Astragaloside Attenuates Dextran Sulfate Sodium (DSS)-Induced Acute Experimental Colitis by Alleviating Gut Microbiota Dysbiosis and Inhibiting NF- κ B Activation in Mice. *Front. Immunol.* **2020**, *11*, 2058. [[CrossRef](#)]
41. Gierynska, M.; Szulc-Dabrowska, L.; Struzik, J.; Mielcarska, M.B.; Gregorczyk-Zboroch, K.P. Integrity of the Intestinal Barrier: The Involvement of Epithelial Cells and Microbiota—A Mutual Relationship. *Animals* **2022**, *12*, 145. [[CrossRef](#)]
42. Fang, J.; Wang, H.; Zhou, Y.; Zhang, H.; Zhou, H.; Zhang, X. Slimy partners: The mucus barrier and gut microbiome in ulcerative colitis. *Exp. Mol. Med.* **2021**, *53*, 772–787. [[CrossRef](#)]
43. Qin, D.; Ma, Y.; Wang, Y.; Hou, X.; Yu, L. Contribution of *Lactobacilli* on Intestinal Mucosal Barrier and Diseases: Perspectives and Challenges of *Lactobacillus casei*. *Life* **2022**, *12*, 1910. [[PubMed](#)]
44. Rodriguez-Pineiro, A.M.; Johansson, M.E. The colonic mucus protection depends on the microbiota. *Gut Microbes* **2015**, *6*, 326–330. [[CrossRef](#)]
45. Zhao, B.; Xia, B.; Li, X.; Zhang, L.; Liu, X.; Shi, R.; Kou, R.; Liu, Z.; Liu, X. Sesamol Supplementation Attenuates DSS-Induced Colitis via Mediating Gut Barrier Integrity, Inflammatory Responses, and Reshaping Gut Microbiome. *J. Agric. Food Chem.* **2020**, *68*, 10697–10708. [[CrossRef](#)] [[PubMed](#)]
46. Vanden Bussche, J.; Marzorati, M.; Laukens, D.; Vanhaecke, L. Validated High Resolution Mass Spectrometry-Based Approach for Metabolomic Fingerprinting of the Human Gut Phenotype. *Anal. Chem.* **2015**, *87*, 10927–10934. [[CrossRef](#)] [[PubMed](#)]
47. Wang, J.; Han, X.; Li, J.; Shi, R.; Liu, L.; Wang, K.; Liao, Y.; Jiang, H.; Zhang, Y.; Hu, J.; et al. Differential analysis of intestinal microbiota and metabolites in mice with dextran sulfate sodium-induced colitis. *World J. Gastroenterol. WJG* **2022**, *28*, 6109–6130. [[CrossRef](#)] [[PubMed](#)]
48. Zhu, G.; Wu, X.; Jiang, S.; Wang, Y.; Kong, D.; Zhao, Y.; Wang, W. The application of omics techniques to evaluate the effects of Tanshinone IIA on dextran sodium sulfate induced ulcerative colitis. *Mol. Omics* **2022**, *18*, 666–676. [[CrossRef](#)]
49. Yuan, Z.; Yang, L.; Zhang, X.; Ji, P.; Hua, Y.; Wei, Y. Mechanism of Huang-lian-Jie-du decoction and its effective fraction in alleviating acute ulcerative colitis in mice: Regulating arachidonic acid metabolism and glycerophospholipid metabolism. *J. Ethnopharmacol.* **2020**, *259*, 112872. [[CrossRef](#)]
50. Zhu, S.; Han, M.; Liu, S.; Fan, L.; Shi, H.; Li, P. Composition and diverse differences of intestinal microbiota in ulcerative colitis patients. *Front. Cell. Infect. Microbiol.* **2022**, *12*, 953962. [[CrossRef](#)] [[PubMed](#)]

Disclaimer/Publisher's Note: The statements, opinions and data contained in all publications are solely those of the individual author(s) and contributor(s) and not of MDPI and/or the editor(s). MDPI and/or the editor(s) disclaim responsibility for any injury to people or property resulting from any ideas, methods, instructions or products referred to in the content.